

## Inconsistent $K$ - $L$ x-ray angular correlations in uranium

T. Papp,\* J. A. Maxwell, W. J. Teesdale, and J. L. Campbell

*Guelph-Waterloo Program for Graduate Work in Physics, University of Guelph, Guelph, Ontario, Canada N1G 2W1*

(Received 10 April 1992)

Angular correlations between  $K\alpha_1$  x rays and subsequent  $L_3$  x-ray transitions were measured using a  $^{233}\text{Pa}$  radionuclide source and high-resolution x-ray detectors. The results provide separately the values of  $A_{22}(K\alpha_1-L\alpha_1)$  and  $A_{22}(K\alpha_1-L\alpha_2)$  as opposed to the compound quantity  $A_{22}(K\alpha_1-L\alpha)$ . For the  $L_1$  and  $L_2$  transitions, the  $A_{22}$  values agreed closely with those based upon theoretical (Hartree-Fock)  $E1$  and  $M2$  transition rates. For the less intense  $L\beta_6$  and  $L\beta_{2,15}$  transitions, agreement was also observed, although within larger uncertainties. In contrast, the value of  $A_{22}(K\alpha_1-L\alpha_1)$  was  $0.085 \pm 0.007$ , which is somewhat larger than the predicted value of 0.073. Possible causes for this discrepancy are explored.

PACS number(s): 32.30.Rj

### I. INTRODUCTION

The predominant lines in the  $K$  and  $L$  x-ray series emitted by an excited atom having an inner-shell vacancy are of electric dipole ( $E1$ ) nature with a very small magnetic quadrupole ( $M2$ ) admixture. Less intense lines are magnetic dipole ( $M1$ ) or electric quadrupole ( $E2$ ) in nature. Scofield's tabulation [1] of relativistic Hartree-Slater transition rates for the radiative filling of  $K$ - and  $L$ -shell vacancies provides the  $M2$ -to- $E1$  intensity ratios ( $\delta^2$ ) for the electric dipole transitions. The presence of  $M2$  radiation causes only a very slight change in the transition rate for  $E1$  x rays. In contrast the effect of an  $M2$  admixture upon the angular correlation between successive x rays in a cascade is significant and measurable. This offers a means of testing the theoretical predictions of multipole admixtures.

The angular correlation function  $W(\theta)$  for successive  $K$  and  $L$  x rays emitted with angle  $\theta$  between them is

$$W(\theta) = W_0 [1 + A_{22} P_2(\cos\theta)], \quad (1)$$

where  $P_2$  is the second-order Legendre polynomial, and the coefficient  $A_{22}$  depends only on the angular momenta and the multipole admixtures  $\delta$ . For the  $2p_{1/2}$  intermediate state ( $L_2$  x rays)  $A_{22}$  is zero. For the  $2p_{3/2}$  intermediate state ( $L_3$  x rays), Scofield provides a full tabulation of the  $A_{22}$  values. It is because these expressions contain  $\delta$  as well as  $\delta^2$  that they are significant, despite the fact that  $\delta^2$  is small compared to unity.

An extensive set of measurements [2] of the angular correlation between  $K\alpha_1$  x rays and various  $L$  x rays has been carried out by various workers, using a coincidence technique based on two semiconductor x ray spectrometers. The available energy resolution limited the  $L$  x rays studied to the  $L_1$  line ( $L_3M_1$ ), the unresolved  $L\alpha$  doublet ( $L_3M_{4,5}$ ), and the  $L\beta$  group (including many unresolved  $L_2$  and  $L_3$  transitions). The measured angular correlations (Fig. 1) agree reasonably well with theoretical predictions for the  $K\alpha_1-L\alpha_{1,2}$  case, but in the  $K\alpha_1-L_1$  case there is evidence, albeit within large error bars, for a discrepancy. Since the value of  $A_{22}(K\alpha_1-L_1)$  is typically

an order of magnitude larger than that of  $A_{22}(K\alpha_1-L\alpha_{1,2})$ , this disagreement cannot be neglected. A similar disagreement has been found in the case of the anisotropies of the  $L_1$  and  $L\alpha$  x rays emitted following proton impact [3]. The experimental  $A_{22}(K\alpha_1-L_1)$  values are generally less than or close to 0.25, a value which would obtain if  $M2$  mixing were negligible. Since the calculated mixing [1] for  $K\alpha_1$  is an order of magnitude larger than that for  $L_1$ , any  $M2$  admixture would increase the value of the expected anisotropy parameter relative to the value 0.25, and this effect would be atomic number dependent as shown in Fig. 1. The discrepancy evident in Fig. 1 might be explained in terms of some effect which causes a dealignment. However, the theoretical extrema of the alignment parameter were observed in impact parameter dependent measurements on dysprosium [4], which tends to exclude the presence of any dealignment mechanism.

The present work was undertaken to check the reported data using the much higher-resolution x-ray detectors and sophisticated spectrum fitting techniques now available, and to extend them to a larger number of  $K$ - $L$  cascades. A particular objective was to separate the  $L\alpha_1$  and  $L\alpha_2$  lines and hence obtain the two correlation parameters instead of a linear combination of them; it was also of interest to ascertain whether the  $K\alpha_1-L_3N_1$  transition cascade emulated the departure from theory of the  $K\alpha_1-L_3M_1$  cascade. The measurement technique is a derivative of that used in our  $K$ -x-ray- $L$ -x-ray coincidence measurements [5] of the Coster-Kronig transition probability  $f_{23}$ .

### II. EXPERIMENTAL DETAILS

#### A. Source and detectors

An x-ray emitter of high atomic number was desired since  $\delta^2$  is largest at high  $Z$  and since the energy separation of  $L$  x-ray lines is greatest. The source chosen was the radionuclide  $^{233}\text{Pa}$  which decays to  $^{233}\text{U}$  with a 27-day half-life providing uranium x rays by internal conversion of nuclear electromagnetic transitions. It was most con-

venient to prepare the source by thermal neutron irradiation of a metallic thorium foil of thickness  $1 \text{ mg/cm}^2$  and area approximately  $6 \text{ mm}^2$ . This irradiation had duration of 50 h with a flux of  $2 \times 10^{13} \text{ s}^{-1} \text{ cm}^2$  producing the radionuclide  $^{233}\text{Th}$ , which decays with 22-min half-life to the desired  $^{233}\text{Pa}$ . The finite thickness of such a foil source necessitates self-absorption corrections for the  $L$  x rays. The uniform thickness renders these accurately calculable, which would not be the case in a source prepared via the more usual technique of drying deposited droplets of a radioactive solution on a thin backing. Another consequence of the finite thickness is the pres-

ence in the measured spectra of thorium  $L$  x rays excited by  $\beta$  particles.

The angular correlation system comprised a fixed Si(Li) detector for the  $L$  x rays and a moving HPGe detector for the  $K$  x rays, with the source carefully located between them so as to lie on the axis of both. The axial location was optimized by measuring the effect of small source displacements off the axis upon x-ray counting rates. The HPGe detector could be rotated to provide  $\theta$  values of  $90^\circ$ – $270^\circ$ , with the source precisely at the center of rotation. The decision to maintain the source and the Si(Li) detector in fixed position eliminates an angle-dependent correction for  $L$  x-ray attenuation in the source foil; only a constant correction is required. This is important since the objective of the work is the most accurate possible determination of angular correlation effects that for some of the transitions are quite small.

To minimize the attenuation [6] of measured angular correlation that arises from the finite solid angle subtended at each detector one has a choice of using collimators at each detector to restrict the solid angle or adopting large source to detector distances to minimize the solid angles. With distances of 6.1 and 3.6 cm, respectively, to the HPGe and Si(Li) detectors, the incidence of  $\gamma$ -ray and  $K$  x-ray scattering off one detector into the other was minimized. A 3-mm-diameter collimator in front of the Si(Li) detector provided the desired angular resolution and screened off the periphery of the detector where poor charge collection adversely affects the line shape. The geometrical dealignment correction was calculated [6] as 1.036.

The planar HPGe detector, fabricated by Aptec Inc., had thickness 10 mm and diameter 20 mm. It was equipped at our request with a 0.5-mm beryllium window of unusually large diameter, viz., 75 mm. This window comprised essentially the entire front face of the cryostat, thus minimizing scattering of  $K$  x rays and subsequent degraded events in the spectrum. The energy resolution at 122-keV energy was 530 eV [full width at half maximum (FWHM)]. The Si(Li) detector, manufactured by Link Analytical plc had thickness 3 mm; an internal tantalum collimator defined its effective diameter as 5 mm. The beryllium window thickness was 0.008 mm and the energy resolution (FWHM) 133 eV at 5.9 keV. These two detectors were chosen for their excellent line-shape characteristics, which in each case has been discussed elsewhere [7,8]. Each has minimal low-energy tailing on the spectral peaks, which is a fundamental requirement for reliable separation of the lines of interest in both the  $K$  and  $L$  x-ray spectra.

### B. Electronic coincidence system

The electronic system that we have described before [5] had to be modified to be compatible with the Link 2040 pulse processor and in addition it was updated so that all coincidence events could be recorded in list mode on the disk of an 80286 computer.

A fast timing signal was obtained from the HPGe detector by the standard means of triggering a constant fraction discriminator (Ortec 473) by the preamplifier

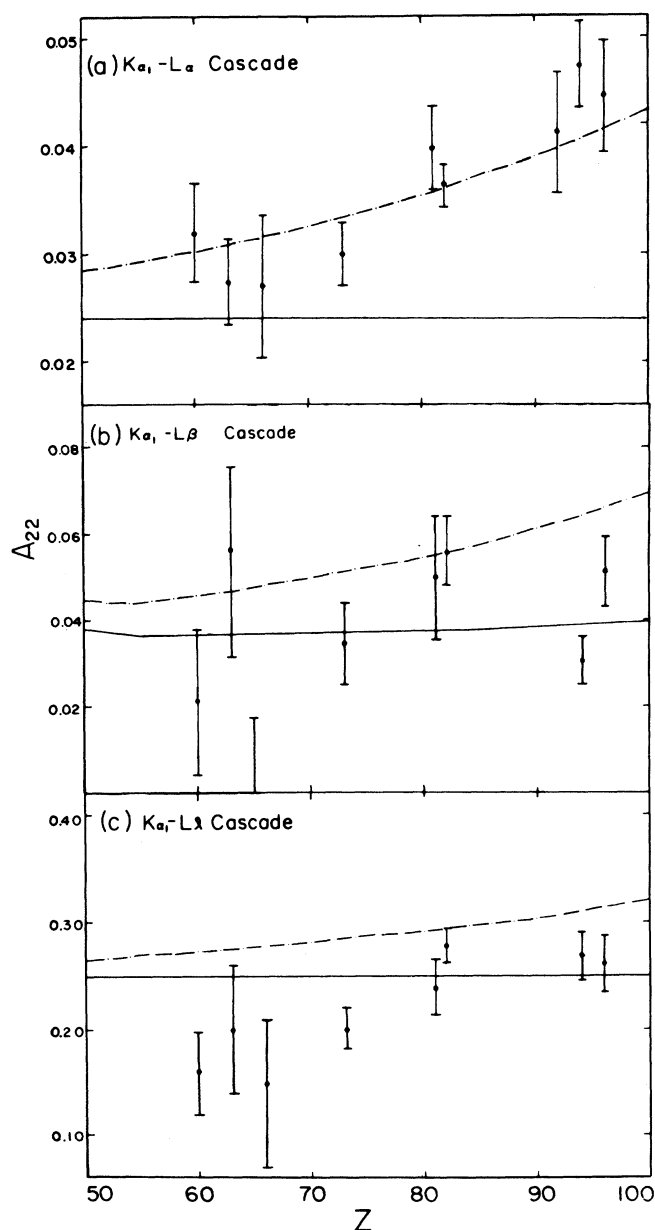


FIG. 1. Summary of measured [2] and predicted [1] angular-correlation coefficients for  $K\alpha_1$ - $L$  x-ray cascades. The dashed curve is based upon the predicted  $M2$ - $E1$  admixtures; the full curve was calculated assuming no admixtures.

pulse, which was first passed through a timing filter amplifier (Ortec 474). The Link preamplifier does not supply a suitable pulse for fast timing, and so the preamplifier pulse was extracted from the processor analog section (at test point 3) and fed through a 100- $\Omega$  resistor to an Ortec 474 timing filter amplifier which fired an Ortec 473 constant fraction discriminator. The  $K$  x-ray discriminator started and the  $L$  x-ray discriminator stopped an Ortec 467 time-to-amplitude converter, which provided a timing pulse ( $T$ ). The large  $K$  x-ray rate in the  $L$  x-ray detector occupied the electronics with unwanted events and so a second discriminator, set to trigger at 32 keV, was placed in parallel with the first and used to inhibit the time-to-amplitude converter.

The two energy pulses ( $L, K$ ) and the time pulse ( $T$ ) were fed to Nuclear Data 575 analog-to-digital converters. A problem arises because the long processing time of the Link 2040 pulse processor results in the  $L$  events arriving some 25  $\mu$ s later than  $K$  and  $T$ . Locally designed 21- $\mu$ s delay amplifiers supplemented by Ortec 427 delay amplifiers (4  $\mu$ s) were used in the  $K$  and  $T$  channels to synchronize the arrival of the  $K$ ,  $T$ , and  $L$  signals at the three ADC's. Each ADC operated in coincidence mode, gated by a logic pulse derived from the time-to-amplitude converter. Since the experiments were of several weeks duration and accurate fitting was necessary, digital stabilizers were attached to the  $K$  and  $L$  ADC's. The three ADC's were connected to a Nuclear Data List module

whose output was read by a Contec P10 96 W input-output (I/O) board housed in an 80286 microcomputer.

Each event ( $K, L, T$ ) presented to the I/O board was recorded in memory, and blocks of 500 events transferred to disk as they were filled; 1800 records were collected at each angle. The computer software provided continuous updating of reconstructed  $L$  x-ray spectra in coincidence with preselected energy windows in the  $K$  x-ray energy spectrum and with windows in the time spectrum.

Twelve runs were performed at 10 angles in the range 90°–180°, the angles being chosen in random order. Each run was of longer duration than its predecessor, in order to achieve the same statistical accuracy despite the decay of the source. In addition several  $K$  x-ray single-event spectra were accumulated to high statistical accuracy. In each of the real coincidence spectra (whose analysis is described below), 5000  $L$  x-ray counts were accumulated at each angle. This was necessary to provide a stringent test of the previously reported deviation [2] between measured and predicted values of  $A_{22}(K\alpha_1-L\alpha)$ . Some examples of spectra are in Fig. 2.

### III. ANALYSIS OF THE DATA

#### A. Analysis of the $K$ x-ray spectra

It was established in our earlier work [7] that the HPGe response to monoenergetic radiation was very well described by the Hypermet function which comprises a Gaussian with a low-energy exponential tail and a flat shelf extending also from the peak centroid to lower energies; these tailing features are convoluted (analytically) with a unit-area Gaussian to remove nonphysical sharp edges. If this function is  $F(i)$ , where  $i$  is the channel number, then a  $K$  x-ray line is

$$K(i) = F(i) * L(i), \quad (2)$$

where the Lorentzian

$$L(i) = \frac{\Gamma/2\pi}{(i-i_0)^2 + (\Gamma/2)^2} \quad (3)$$

describes the intrinsic shape of the x-ray line.

The  $K\alpha$  x-ray triplet measured in single-event mode was fitted with the sum of three such convolutes, superposed on a polynomial background, using a nonlinear least-squares code [7]. These convolutes represent the two intense electric dipole lines  $K\alpha_1$  and  $K\alpha_2$  and the weak magnetic dipole line  $K-L_1$  (whose intensity relative to  $K\alpha_1$  is approximately  $10^{-3}$ ). The energies [9] and Lorentzian widths [10] of the three peaks were fixed, and their heights, together with the height and slope parameters of the low-energy tailing feature, treated as variables which were determined by the fit. Energy windows were then established to define the  $K\alpha_2$ ,  $K\alpha_1$ , and  $K\beta$  regions and continuum regions above  $K\alpha$  ( $A-K\alpha$ ) and above  $K\beta$  ( $A-K\beta$ ); the window limits corresponded to the full width at tenth maximum of the respective peaks. From the fit, the precise contribution of peaks, tails, and continuum background to each window was determined.

Windows were also established in the overall time spec-

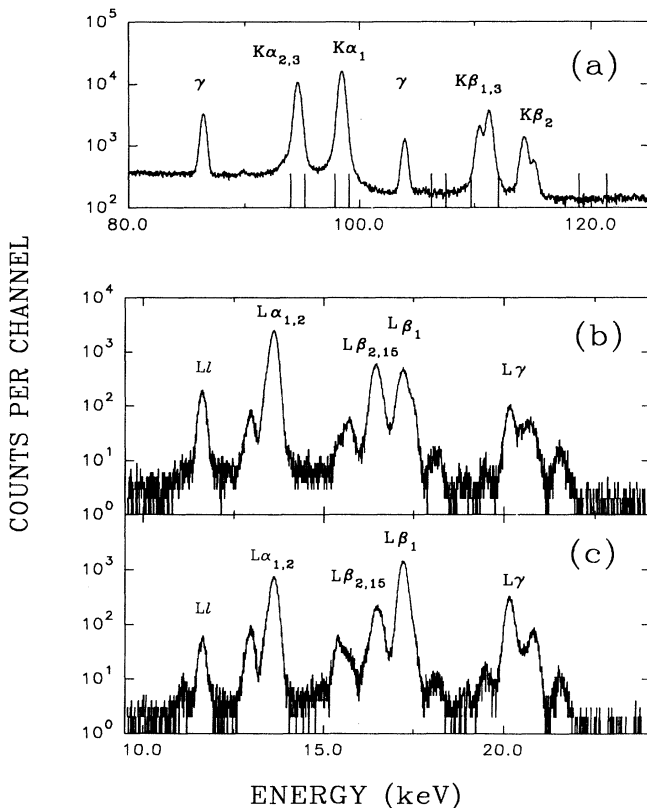


FIG. 2. Measured x-ray spectra: (a) single-event  $K$  x-ray spectrum; (b)  $L$  x-ray spectrum coincident with  $K\alpha_1$  x rays only; (c)  $L$  x-ray spectrum coincident with  $K\alpha_2$  x rays only.

trum recorded during the  $K$ - $L$  coincidence experiment, defining regions of real plus random and of random coincidence events.

### B. Analysis of the $L$ x-ray coincidence spectra

The objective here is to separate out the intensities of as many individual  $L$  x-ray lines as possible in the coincident  $L$  x-ray spectra taken at the various angles. As in the  $K$  single-event case this involves a nonlinear least-squares fit, which relies upon the known line shapes. The line energies are known [9] and may be fixed in the fit. The line shape has been determined experimentally [8] using monoenergetic radiation provided by a curved crystal monochromator, and this work has shown that for the present Si(Li) detector used in collimated mode the low-energy tailing additives to the main Gaussian component are very small. However, the  $L$  x rays from the radioactive source are not monoenergetic but have intrinsic Lorentzian distributions whose widths  $\Gamma$  are non-negligible and as a result cause significant tailing on both the low- and high-energy sides of the peaks. It is imperative that this effect, invariably neglected in Si(Li) work reported in the literature, be taken into account in any attempt to achieve an accurate fit to a measured  $L$  x-ray spectrum from an atom of high atomic number.

The magnitude of these Lorentzian effects is demonstrated in Fig. 3. Here the  $Ll$  and  $L\alpha$  region of a uranium  $L$  x-ray spectrum measured in single-event mode is fitted first with Gaussian and then with Gaussian-Lorentzian convolutes representing the full-energy peaks. The need for the convolutes is clear, as we have also demonstrated [11] using  $L$  x-ray spectra from proton impact on thorium metal foils. We obtained 26.6 and 13.3 eV for the Lorentzian widths of the  $Ll$  and  $L\alpha_1$  lines, respectively. The intensity ratio of the overlapping  $L\alpha_1$  and  $L\alpha_2$  components of the  $L\alpha$  doublet was  $0.115 \pm 0.003$ ; this is in excellent agreement with Scofield's theoretical prediction [1] of 0.114. This ratio was also determined from the  $L$  x-ray coincidence spectra, with the Lorentzian widths fixed at the values obtained above. In this case it is the ratio of the  $W_0$  parameters of the  $L\alpha_2$  and  $L\alpha_1$  transitions obtained from the fits to the angular distributions using the function of Eq. (1); this result was  $0.115 \pm 0.001$ .

In fitting the  $L$  x-ray coincidence spectra coincident with  $K\alpha_2$  and  $K\alpha_1$ , the necessary Lorentzian widths were taken from the review of Salem and Lee [13] except for the  $Ll$ ,  $L\alpha_2$ , and  $L\alpha_1$  lines, where our own measurements, based on fits to single-event spectra measured to intensities of  $10 \times 10^6$  counts, were used. The intensities of the silicon  $K$  x-ray escape peak, a necessary part of the computed model spectrum, were based on the parametrization of Johansson [14].

The  $K\alpha_1$ - $L$  coincidence spectrum (after the various corrections described below) contains only  $L_3$  x-ray lines, each of which is expected to show a distinct angular correlation. The  $K\alpha_2$ - $L$  coincidence spectrum (similarly corrected) contains mainly  $L_2$  x-ray lines, and these are expected via elementary quantum mechanics to be isotropic, which provides a useful normalization. The intensi-

ties of the  $K\alpha_1$ - $L_3$  lines are expressed as multiples of these of the  $K\alpha_2$ - $L_2$  lines. Corrections have been applied to each  $L$  x-ray line intensity to account for detector efficiency and for attenuation both in air and in the source foil.

### C. Reduction of the coincidence data

The least-squares fit to the  $L\alpha$  and  $L\beta$  regions of the  $L$  x-ray coincidence spectra provided various individual  $L$  x-ray line intensities coincident with  $K$  x-ray events in the five windows selecting  $K\alpha_2$ ,  $K\alpha_1$ ,  $A$ - $K\alpha$ ,  $K\beta$ , and  $A$ - $K\beta$ .

We trace the analysis for a single  $L$  x-ray line, denoted  $L_i$ , at angle  $\theta$ . Subtraction of the five random coincidence intensities from the five real-plus-random intensities leaves the real coincidence intensities. These five numbers do not correspond exactly to the  $K$  x-ray event type that designates each of the five windows; they must be corrected to remove  $L_i$  x-ray events in coincidence with minor contributions to the windows. The contributions due to  $A$ - $K\alpha$  events in the  $K\alpha_1$  and  $K\alpha_2$  windows and due to  $A$ - $K\beta$  events in the  $K\beta$  window were removed by subtracting appropriately normalized  $L_i$  x-ray intensities in coincidence with  $A$ - $K\alpha$  and  $A$ - $K\beta$  from those coincident with  $K\alpha_2$ ,  $K\alpha_1$ , and  $K\beta$ , leaving three surviving  $L_i$  x-ray intensities.

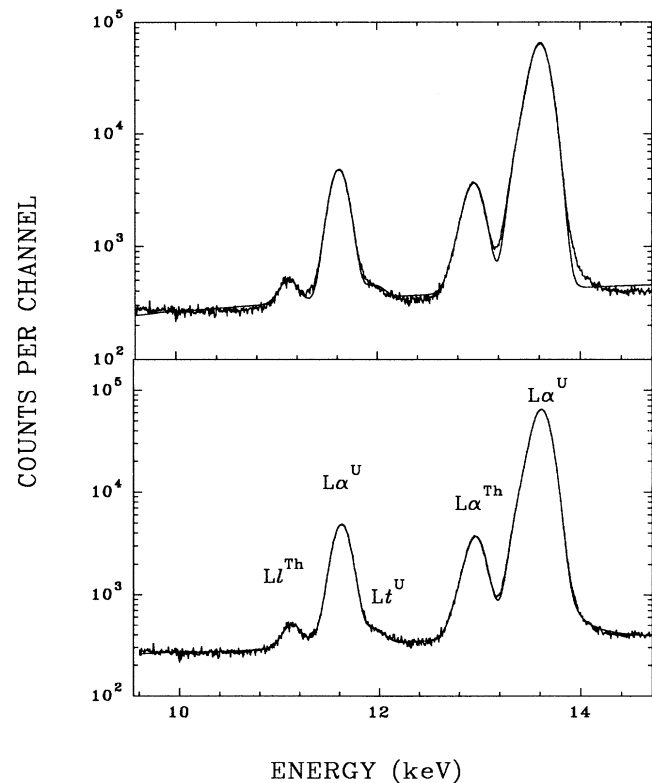


FIG. 3. Fits to part of an  $L$  x-ray spectrum containing the  $Ll$  and  $L\alpha$  lines of uranium and thorium. The upper fit used a Gaussian shape for the full-energy peaks and the lower used Lorentzian-Gaussian convolutes. The uranium  $L_i$  line can be seen at 11.98-keV energy.

The next analysis step is necessitated by the fact that these are two distinct classes of real  $K$  x-ray- $L$  x-ray events. The first of these, the one of interest, comprises events where  $K$  x-ray emission arising from  $K$  internal conversion is followed by  $L$  x-ray emission in the same atom. However, some of the electromagnetic transitions in the daughter  $^{233}\text{U}$  nucleus are in cascade and so  $K$  and  $L$  x rays from sequential internal conversions are also recorded as coincidences. While these are real coincidences relative to the approximately 50-ns resolving time of the electronic system, they are, in fact, well separated on the atomic time scale; the  $K$  vacancy lifetime is of order  $10^{-16}$  s and the nuclear lifetimes  $10^{-12}$ - $10^{-9}$  s, so that the first ( $K$  or  $L$ ) vacancy is filled long before the second nuclear transition occurs. We refer to these as unrelated coincidences. This class of events will also include those involving an x ray from internal conversion and a second x ray arising from fluorescence or  $\beta$ -particle ionization.

$K\beta$  x rays, which do not result in  $L$  vacancies, are observed in real coincidence with  $L$  x rays. Such events can only arise from unrelated coincidences and they provide a means to correct for events of this class in the two  $L_i$  x-ray intensities coincident with  $K\alpha_2$  and  $K\alpha_1$ . The  $L_i$  x-ray intensity coincident with  $K\beta$  is normalized successively by the  $K\alpha_2:K\beta$  and  $K\alpha_1:K\beta$  intensity ratios from the single-event  $K$  x-ray spectrum fit; these contributions are then subtracted off the  $K\alpha_2$ - and  $K\alpha_1$ -coincident intensities. We find that 26.4% of the coincidence events are of the unrelated type. This results, for  $L_3$  x rays, in a correction factor of  $1.359 \pm 0.006$  to the measured  $A_{22}$  values. This number is in excellent agreement with the earlier work of Catz and Finkel [12] on the same nuclide.

As a result of this fairly laborious procedure we have at each angle the various  $L_i$  x-ray intensities coincident with  $K\alpha_1$  events, together with a statistical uncertainty propagated through the calculation. The correction due to  $K\alpha_2$  events in the  $K\alpha_1$  window is negligible.

#### IV. RESULTS AND DISCUSSION

The measured angular correlations are presented in Fig. 4; as indicated earlier they have been calculated by using  $L_3$  line intensities relative to the  $K\alpha_2$ - $L_2$  intensity, which is expected to be isotropic. A test to ascertain that the latter is indeed the case is provided by the ratio of the  $L_2$ -coincident x-ray intensity to the overall counting rate of  $K$  x rays (monitored by a scaler connected to the computer's I/O board) which is indeed isotropic. The  $A_{22}$  values derived from linear least-squares fits to the measured correlation functions are compared with the Dirac-Hartee-Slater predictions of Scofield [1] in Table I. These predictions are based upon the multipole mixing ratio  $\delta$  given by Scofield's calculations. The quoted errors of the angular correlation parameters are the standard deviation values obtained from the least-squares fitting of Eq. (1) to the measured angular correlations. The measured intensities were weighted with the inverse square of their one standard deviation errors obtained from the fitting of the  $L$ -shell spectra supposing Poisson counting statistics. The statistical error of the  $K\alpha$  events was negligible.

Our  $K\alpha_1$ - $L_1$  result is in good agreement with the theoretically predicted angular correlation parameter. This result may be compared with earlier data for atomic numbers between 80 and 100, most of which lie slightly below the prediction (dashed curve in Fig. 1). The present result, however, has considerably better precision than the earlier ones.

Our data provide separate  $A_{22}$  values for the cascades  $K\alpha_1$ - $L\alpha_2$  and  $K\alpha_1$ - $L\alpha_1$ . The extremely good agreement between theory [1] and our measured  $I(L\alpha_2)/I(L\alpha_1)$  intensity ratio lends strong support to these results. While  $A_{22}(K\alpha_1-L\alpha_2)$  is in close agreement with theory,  $A_{22}(K\alpha_1-L\alpha_1)$  is larger than the predicted value. We would have expected any fitting error to affect primarily the less intense ( $\times 10$ ) component  $L\alpha_2$ , and so the agree-

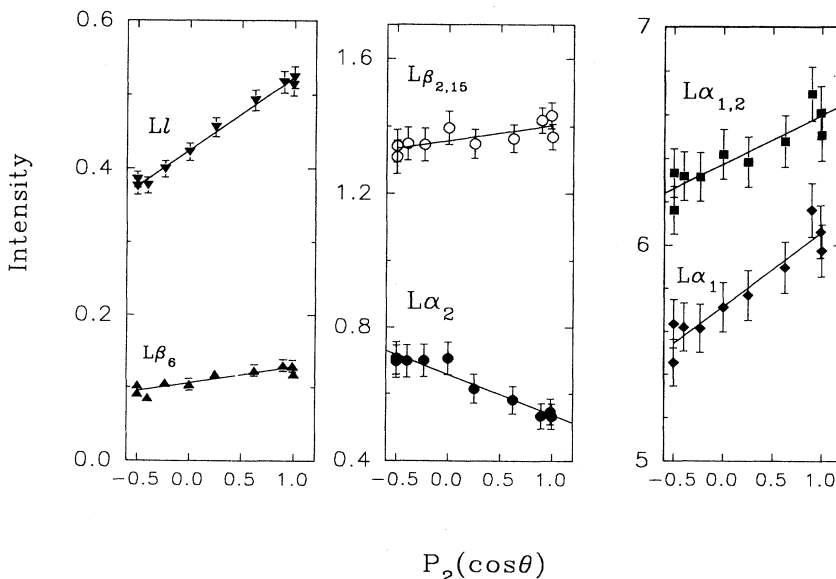


FIG. 4. Measured angular correlation functions for  $K\alpha_1$ - $L$  cascades in uranium. The intensity of each  $L$  x-ray line is expressed relative to that of the  $K\alpha_2$ - $L_2$  x-ray cascade, which is isotropic.

TABLE I. Angular correlation parameters for  $^{233}\text{U}$ .

Transition	$A_{22}$		
	Measured	Corrected <sup>a</sup>	Theory [1]
$K\alpha_1-Ll$	0.225±0.008	0.316±0.011	0.3053
$K\alpha_1-L\alpha_2$	-0.181±0.012	-0.255±0.016	-0.2536
$K\alpha_1-L\alpha_1$	0.060±0.005	0.085±0.007	0.0735
$K\alpha_1-L\alpha_{1,2}$	0.036±0.005	0.050±0.007	0.0405
$K\alpha_1-L\beta_6$	0.205±0.036	0.288±0.050	0.3020
$K\alpha_1-L\beta_{2,15}$	0.034±0.007	0.048±0.010	0.0427
$K\alpha_2-Ll$	0.002±0.007		
$K\alpha_2-L\alpha_{1,2}$	0.006±0.009		
$K\alpha_2-L\beta_1$	0.001±0.005		
$K\alpha_2-L\gamma_1$	0.006±0.007		
$K\beta_{1,3}-Ll$	0.000±0.001		
$K\beta_{1,3}-L\alpha_{1,2}$	0.005±0.005		

<sup>a</sup>Correction factors of 1.359 and 1.036 are applied for unrelated coincidences and geometrical dealignment.

ment of the  $L\alpha_2$  result with theory tends to strengthen the conclusion that the  $L\alpha_1$  result is indeed anomalous. The ratio of the  $A_{22}(K\alpha_1-Ll)$  and  $A_{22}(K\alpha_1-L\alpha)$  is in perfect agreement with the anisotropy parameter ratio of the  $Ll$  and  $L\alpha$  transitions obtained by measuring the angular distribution of these lines following proton impact [15], and the angular correlation ratios following  $\alpha$  decay [16].

The  $L\beta$  group contains several  $L_2$  and  $L_3$  x-ray transitions, which will be isotropic and anisotropic, respectively. It is not surprising therefore that the early measurements shown in Fig. 1(b) show a very large scatter and that no specific conclusions can be drawn. In the present work the  $L\beta_6(L_3N_1)$  line is well resolved, and its  $A_{22}$  value agrees; albeit within  $\pm 17\%$  error bars, with theory. Thus neither the  $L_3M_1(Ll)$  nor the  $L_3N_1(L\beta_6)$  line, each of which involve a final s-state electron, deviate from theory. The  $K\alpha_1-L\beta_{2,15}$  cascade is analogous to the  $K\alpha_1-L\alpha_{1,2}$  case, involving  $N_{4,5}$  final states, which are similar to  $M_{4,5}$ ; however, the precision of the measurement is not sufficient to discern a deviation of the type established for  $A_{22}(K\alpha_1-L\alpha_{1,2})$ .

Table I presents also the  $A_{22}$  parameters for various transition cascades involving  $K\alpha_2$  x rays. As noted earlier these cases should be isotropic, and the null results therefore provide an assurance that systematic angle-dependent errors are not present.

We now return to the discrepancy between measured and predicted values for  $A_{22}(K\alpha_1-L\alpha_1)$ . In the  $K\alpha_1-L\alpha_2$  cascade, the sequence of angular momentum states is  $s_{1/2}p_{3/2}-d_{3/2}$ , and for the  $d_{3/2}\rightarrow p_{3/2}$  transition the

theoretical  $M2$  rate is zero. We can therefore deduce from the measured  $A_{22} = -0.255 \pm 0.016$  a value of  $0.082 \pm 0.023$  for  $\delta_{K\alpha_1}$ , which agrees very closely with the Scofield [1] prediction of 0.0817. If we now accept the Scofield value, it follows from the  $K\alpha_1-L\alpha_1$  result that  $\delta_{L\alpha_1} = 0.029 \pm 0.009$ , which deviates more than one standard deviation from Scofield's calculated value of 0.0130. One possible conclusion is therefore that the theoretical  $K\alpha_1$  multipole admixture is correct but that for  $L\alpha_1$  the theory underestimates the actual value (while giving the correct value for  $Ll$  and  $L\alpha_2$ ).

This conclusion is unappealing in terms of consistency. It may therefore be worthwhile to note that the  $M2$ -to- $E1$  mixing ratios were calculated via Hartree-Slater [1] theory, whereas the angular correlation parameters were obtained using the formalism of [15] assuming the independent electron model. The observed deviation between theoretical and experimental results may be indicative of a breakdown of the independent electron model in the description of angular distribution and angular correlation of x rays. In addition it should be noted that the ratio of  $A_{22}$  values for the  $K\alpha_1-Ll$  and  $K\alpha_1-L\alpha$  cascades agrees with previous data from proton impact [16] and  $\alpha$  decay [17], which depart from the theoretical predictions. These observations obviously merit further investigation.

#### ACKNOWLEDGMENTS

We thank the Natural Sciences and Engineering Research Council for financial support. We are grateful to E. S. Macias for permission to use Fig. 1.

\*On leave from the Institute of Nuclear Research of the Hungarian Academy of Sciences (ATOMKI) Debrecen, H-4001, Pf.51 Hungary.

[1] J. H. Scofield, Lawrence Livermore Laboratory Report No. UCRL-51231 (1972) (unpublished); *Atomic Inner Shell Processes*, edited by B. Crasemann (Academic, New York,

1975), p. 265.

[2] E. S. Macias and M. R. Zalutsky, *Phys. Rev. A* **9**, 2356 (1974).

[3] T. Papp, Y. Awaya, A. Hitachi, T. Kambara, Y. Kanai, T. Mizogawa, and I. Török, *J. Phys. B* **24**, 3797 (1991).

[4] F. Konrad, R. Schuch, R. Hoffman, and H. Schmidt-

- Böcking, Phys. Rev. Lett. **52**, 188 (1984).
- [5] P. L. McGhee and J. L. Campbell, J. Phys. B **21**, 2295 (1988).
- [6] J. L. Black and W. Gruhle, Nucl. Instrum. Methods **46**, 213 (1967).
- [7] J. L. Campbell, P. L. McGhee, J. A. Maxwell, R. W. Ollerhead, and B. Whittaker, Phys. Rev. A **33**, 986 (1986).
- [8] J. L. Campbell and J. X. Wang, X-Ray Spectrom. **20**, 191 (1991).
- [9] *Table of Isotopes*, edited by C. M. Lederer and V. S. Shirley (Wiley, New York, 1978).
- [10] M. O. Krause and J. H. Oliver, J. Phys. Chem. Ref. Data **8**, 329 (1979).
- [11] T. Papp, J. L. Campbell, J. A. Maxwell, J.-X. Wang, and W. J. Teesdale, Phys. Rev. A **45**, 1711 (1992).
- [12] A. L. Catz and L. Finkel, in *Proceedings of the International Conference on Inner Shell Ionization Phenomena and Future Applications*, edited by R. W. Fink, S. T. Manson, F. M. Palms, and P. Venugapala Rao, U.S.A.E.C. Report No. CONF-720404 (U.S. GPO, Washington, DC, 1973) p. 257.
- [13] S. I. Salem and P. L. Lee, At. Data Nucl. Data Tables **18**, 234 (1976).
- [14] G. Johansson, X-Ray Spectrom. **11**, 194 (1982).
- [15] H. J. Rose and D. M. Brink, Rev. Mod. Phys. **39**, 306 (1967).
- [16] T. Papp, J. Pálincás, and L. Sarkadi, Phys. Rev. A **42**, 5452 (1990).
- [17] P. N. Johnston, Phys. Rev. C **44**, R586 (1991).